RESEARCH PAPER

Bacteriophage 1:3, 165-173; May/June 2011; © 2011 Landes Bioscience

Investigation of bacteriophage T4 by atomic force microscopy

Yuri G. Kuznetsov, Sheng-Chieh Chang and Alexander McPherson*

Department of Molecular Biology and Biochemistry; University of California Irvine; Irvine, CA USA

Key words: DNA, virus, mutants, hoc, soc, capsomeres

Bacteriophage T4 was visualized using atomic force microscopy (AFM). The images were consistent with, and complementary to electron microscopy images. Head heights of dried particles containing DNA were about 75 nm in length and 60 nm in width, or about 100 nm and 85 nm respectively when scanned in fluid. The diameter of hydrated tail assemblies was 28 nm and their lengths about 130 nm. Seven to eight pronounced, right-handed helical turns with a pitch of 15 nm were evident on the tail assemblies. At the distal end of the tail was a knob shaped mass, presumably the baseplate. The opposite end, where the tail assembly joins the head, was tapered and connected to the portal complex, which was also visible. Phage that had ejected their DNA revealed the internal injection tube of the tail assembly. Heads disrupted by osmotic shock yielded boluses of closely packed DNA that unraveled slowly to expose threads composed of multiple twisted strands of nucleic acid. Assembly errors resulted in the appearance of several percent of the phage exhibiting two rather than one tail assemblies that were consistently oriented at about 72° to one another. No pattern of capsomeres was visible on native T4 heads. A mutant that is negative for the surface proteins hoc and soc, however, clearly revealed the icosahedral arrangement of ring shaped capsomeres on the surface. The hexameric rings have an outside diameter of about 14 nm, a pronounced central depression, and a center-to-center distance of 15 nm. Phage collapsed on cell surfaces appeared to be dissolving, possibly into the cell membrane.

Introduction

T4, a double stranded DNA bacteriophage belonging to the family Myoviridae, infects the bacteria *E. coli*. It was one of the first viruses visualized by electron microscopy[1] and its head and tail design first described by Luria and Anderson.[2] It is the most thoroughly characterized bacteriophage and among the most complex, having a prolate icosahedral head (capsid), a contractile tail apparatus for introduction of nucleic acid into the host, tail fibers for cell surface recognition and attachment, and a molecular motor for encapsidating its genome. T4 is among the largest bacteriophages; from electron microscopy, its overall length being about 200 nm.[3-5]

Although T4 has been the subject of innumerable genetic experiments and structural investigations using a host of techniques,[4] it still holds considerable interest to molecular biologists. The detailed structure of its icosahedral head has recently been delineated,[6] its molecular motor is the object of intense study,[7,8] and it is providing a platform for ingenious experiments regarding DNA packaging and release.[9] The various biological and structural aspects of T4 have been thoroughly reviewed in reference 4, and it would not be possible to recount all of them here.

Virtually all of the structural proteins in the virion have been characterized, as were their genes. The major capsid protein, which forms the icosahedral lattice, is designated gp23, but there is a second protein, gp24 which caps each of the 5-fold vertexes. The tail sheath is composed principally of a protein gp18 and the internal injection tube of gp19. The base plate, to which both tail spikes and long sensory fibers are attached, is the most complicated structure in most ways, being composed of about fifteen proteins. It is through short tail spikes (made from gp 10 and gp11) on the underside of the base plate that cell surface attachment occurs. The long tail fibers, which detect receptor molecules on the host cell are also complex and formed from at least four different proteins.[10] The major capsid proteins are not exposed directly to the exterior, but are associated with two smaller proteins of about 10 kD to 13 kD called *hoc* and *soc*.[11,12] Presentation of these proteins defines the exposed surface of T4 and they come into closest approach to the AFM cantilever tip when the capsid is scanned.

A technique that has not been applied to the study of T4 in detail and at high magnification is atomic force microscopy (AFM). AFM has some advantages with respect to other techniques, sometimes providing information not easily obtained by either electron microscopy or even X-ray crystallography. AFM is a single particle technique that is not dependent on properties that are common to a population. It frequently reveals individual eccentricities that otherwise go unnoticed. Its resolution is in the range of a nanometer in the best of cases, and it may be applied

*Correspondence to: Alexander McPherson; Email: amcphers@uci.edu
Submitted: 04/23/11; Revised: 07/16/11; Accepted: 08/06/11
http://dx.doi.org/10.4161/bact.1.3.17650

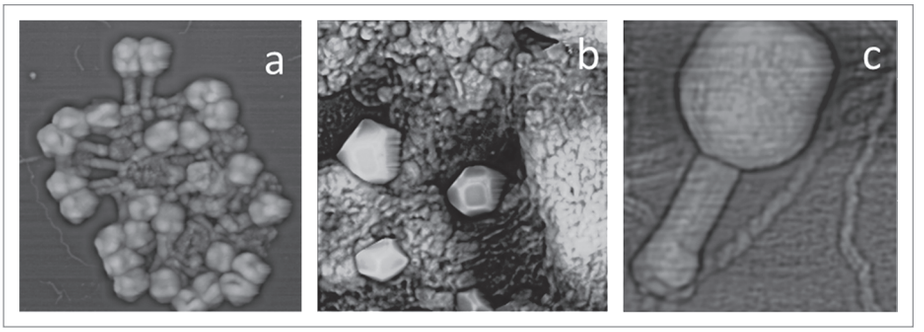

Figure 1. T4 phage, upon drying on the AFM substrate, generally aggregate into clusters as seen in (a), but their distinctive features remain evident. In (b) are phage heads on the surface of an *E. coli* cell. In (c) is a high magnification AFM image of a single T4 phage. The scan sizes and height ranges are respectively (a) 220 nm x 220 nm, 1 μm, (b) 2 μm x 2 μm, 400 nm and (d) 250 nm x 250 nm, 150 nm.

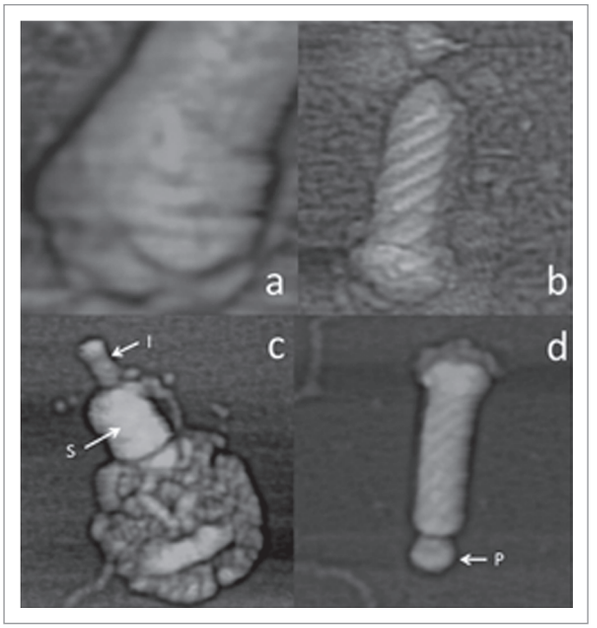

Figure 2. Structural elements of a T4 phage particle. In (a) is an AFM image of the base plate. It assumes an ambiguous, knob shape, likely due to the convolution of the AFM cantilever tip with base plate that rises precipitously above the substrate. In (b) the helical turns characteristic of the T4 phage tail assembly can be seen. The assembly tapers at one end to join with the head through the portal complex and flares at the other end into the base plate seen in (a). In (c) a phage particle that has already injected its DNA has collapsed on the AFM substrate. The compressed tail sheath (S) and the internal injection tube (I) are evident. In (d) a tail assembly has pulled free of a phage head. At the proximal end of the assembly is a is a distinctive structure (P) the portal complex, that couples the tail assembly to the phage head. The scan sizes and height ranges are respectively (a) 110 nm x 110 nm, 50 nm, (b) 150 nm x 150 nm, 120 nm, (c) 250 nm x 250 nm, 60 nm and (d) 200 nm x 200 nm, 70 nm.

to specimens that have been dried in air, or to subjects in liquids, including physiological fluids and biological buffers.[13-16]

We describe here a high resolution investigation of T4 bacteriophage with two objectives. The first is to make a qualitative and quantitative comparison of particle properties and dimensions deduced from AFM images with the same features derived from other methods, particularly electron microscopy. The second is to present several novel observations made possible by AFM that have not been previously reported but that may reshape thinking regarding some aspects of the virus structure.

Results

Morphological features and dimensions: comparison with electron microscopy results. In **Figure 1a** is a mass of T4 virus having the characteristic polyhedral heads that contain 172 kbp of genomic DNA[6] uncomplexed with protein,[9,17] and the contractile tail assemblies for the introduction of the genomic DNA into a host cell. Virus particles interacting with the surfaces of *E. coli* cells were also visualized as in **Figure 2b**. Single particles, like that in **Figure 1c**, attached to the mica substrate were common as well and permitted measurement of particle dimensions in both the dry and fully hydrated state.

Phage heads. The lengths and widths of the heads, measured from air-dried samples, were approximately 75 nm and 60 nm respectively. From hydrated samples we obtained dimensions of about 100 nm and 85 nm respectively. The latter compare well with measures obtained from electron microscopy[18,19] and as measured by X-ray diffraction of solution samples.[20] The smaller dimensions of the dried samples, about 25% to 30% less, are due not only to loss of water, but also to some flattening of the specimens upon drying on the substrate. The percentage difference noted here for the hydrated and dried heads was similar to that seen for other components of the virus and seems to be a consistent feature of the AFM analysis. The length of the tail sheaths of hydrated samples was about 130 nm, again consistent with values from electron microscopy[21] and solution X-ray scattering.[20] The junction between the tail sheath and the head is unadorned in AFM images and displays no collar or neck fibers as were seen using electron microscopy.

The baseplate. The distal end of the tail assembly flares to exhibit a knob-like structure. A higher magnification AFM image is shown in **Figure 2a**. Presumably this is the base plate and connection points for both short and long tail fibers.[10,22,23] Although we rarely saw intact tail fibers on the T4 virus, we often saw fragments of them on the substrate, and fully attached on other tailed phages prepared by different procedures.[24] Likely the fibers were simply broken and lost during the preparation of the phage. The hexagonal baseplate of T4 is always oriented on edge to the AFM probe, which is the worst possible situation for AFM imaging. Convolution of the cantilever tip shape with a plate standing on edge can do no better than yield the ambiguous form in **Figure 2a**.

The tail assembly: helical features. The tail assemblies or sheaths exhibit helical architecture at high magnification, as seen in the AFM image of **Figure 2b**, although they are, in

fact, composed of stacked disks.[18,25,26] The diameter of the tail assemblies is about 28 nm based upon height measurements of fully hydrated samples. This compares with a diameter of 22 nm measured by electron microscopy.[18,27,28] The tails have the appearance of right handed screws with boldly raised threads. We observe there to be 7 to 8 turns of the screw, which have a pitch of about 15 nm. The chirality of the helix, number of turns observed by AFM, and their pitch are also the same as deduced by electron microscopy.[18] The tails are not strictly cylindrical, but like a screw have a taper. The tapered end couples through a portal complex to a specific 5-fold vertex of the polyhedral head.

Although most of the tail assemblies were observed in extended, non-contracted states, we occasionally recorded phage particles which did exhibit contracted sheaths. Contraction of tail assemblies is known to occur under some conditions in the absence of cells or their receptors, for example 1 M NaCl. We suspect that contraction may have been promoted in these cases by the freezing and thawing of virions. The empty heads of these particles collapsed into disorganized shells as a result of drying. Heads containing DNA did not collapse under the same stress, which allowed ready identification of full and vacant capsids.

Phage that had contracted tail sheaths showed that the contraction process reduced the length of the tail sheath to 64 nm, or about a 50% reduction from its extended state. This is again consistent with previous electron microscopy measurements.[18] Exhausted particles also allowed visualization of the injection tube inside, as seen in **Figure 2c**, and a measure of its width of 18 nm. Among the free tail assemblies were some that had been pulled and separated from an associated head, and one is shown in **Figure 2d**. At the proximal, tapered end of the assembly is a discrete structure, which corresponds to the junction with the phage head. We presume this to be the portal complex and motor by which the genomic DNA is drawn into the head.

Additional observations based on the AFM analysis. *The icosahedral heads: hoc and soc Proteins.* We did not observe any regular lattice of protein units, or capsomeres on the polyhedral heads of the particles, as evidenced by **Figures 1, 3a and b**, although a regular lattice based on icosahedral architecture exists below the external surface.[6,18,29-31] It is known, however, that the icosahedral network is coated with *hoc* and *soc*, two small, external proteins of obscure function.[12,29,32,33] These two proteins potentially extend flexible domains that protrude from the surfaces of the heads. Their shielding of the icosahedrally disposed major capsid proteins, and their mobility and potential movement in response to AFM tip pressure likely explains why a periodic network cannot be seen on native capsids.

To test this hypothesis, a mutant of T4 that fails to produce the hoc and soc proteins was grown in a suppressor strain of *E. coli* and examined by AFM in the same manner as was the native phage. As is evident in **Figure 3c and d**, in the absence of the two surface proteins the icosahedral net exhibited by the coat proteins gp23 and gp24 becomes visible. In some AFM images (**Fig. 3c and d**) capsomeres are obvious and even the MCP units of which they are composed are beginning to emerge in **Figure 4**.

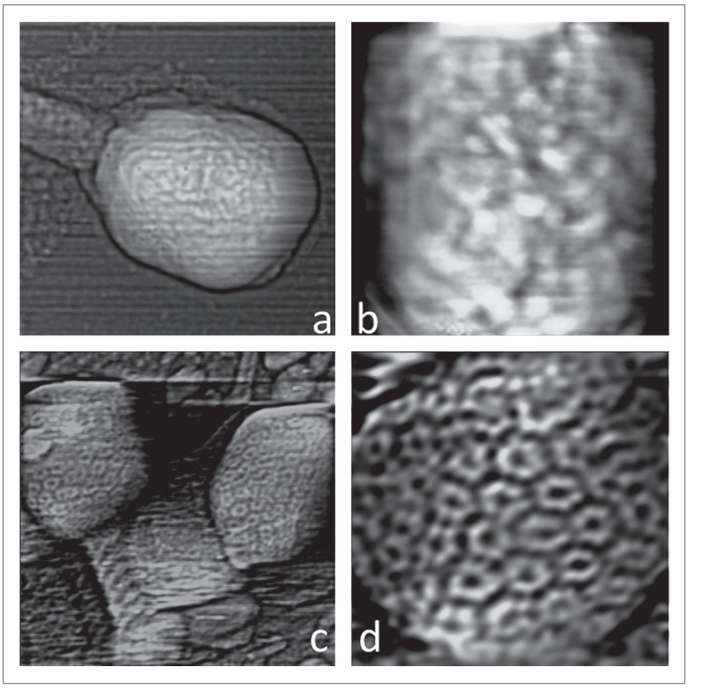

Figure 3. In (a) is a moderate magnification AFM image of a native T4 phage head, comparable to that seen in Figure 1c. In (b) is a higher magnification image of a native phage head. In neither (a) nor (b) are any structural details visible on the surface of the head, nor is it even obvious that the head exhibits icosahedral geometry. In (c and d) are increasingly higher magnification AFM scans of a mutant T4 bacteriophage that fails to express the hoc and soc surface proteins. Unlike the capsids of native T4 seen in (a and b), the mutant capsids clearly display an icosahedral arrangement of capsomeres. The scan sizes and height ranges are respectively (a) 200 nm x 200 nm, 200 nm, (b) 100 nm x 100 nm, 60 nm, (c) 250 nm x 250 nm, 150 nm and (d) 90 nm x 90 nm, 150 nm.

From the AFM images, the capsomeres are ring shaped and protrude somewhat from the virus surface. They have a distinctive depression at their centers. It has been shown that the hoc protein binds at the centers of the hexagonal capsomeres, presumably within the depressions. The center to center distances of the capsomeres in AFM images of fully hydrated particles is 15 nm, and that part of the capsomere that rises up significantly above the basal level of the head has an outside ring diameter of about 14 nm. The gp 23 molecule in the mature head has a molecular weight of 48,000 Daltons,[11] which appears consistent with the sizes of the protein subunits making up the capsomeres.

Collapsed phage capsids. We observed that common accompaniments to intact phage and their various components were the round objects indicated by arrows in **Figure 5a**. These were what we might term sombrero in shape in that they had a dish-like profile, in general, with a rise at their centers. The objects are often associated with a recognizable tail assembly, as in **Figure 5b**, suggesting that they are derived from phage particles. In higher magnification images the objects were marked by distinctive depressions, possibly perforations, that superficially appeared to exhibit some local spatial order, but in fact followed no strict geometrical pattern. The diameters of the objects vary considerably between 150 nm and 250 nm, which are significantly larger

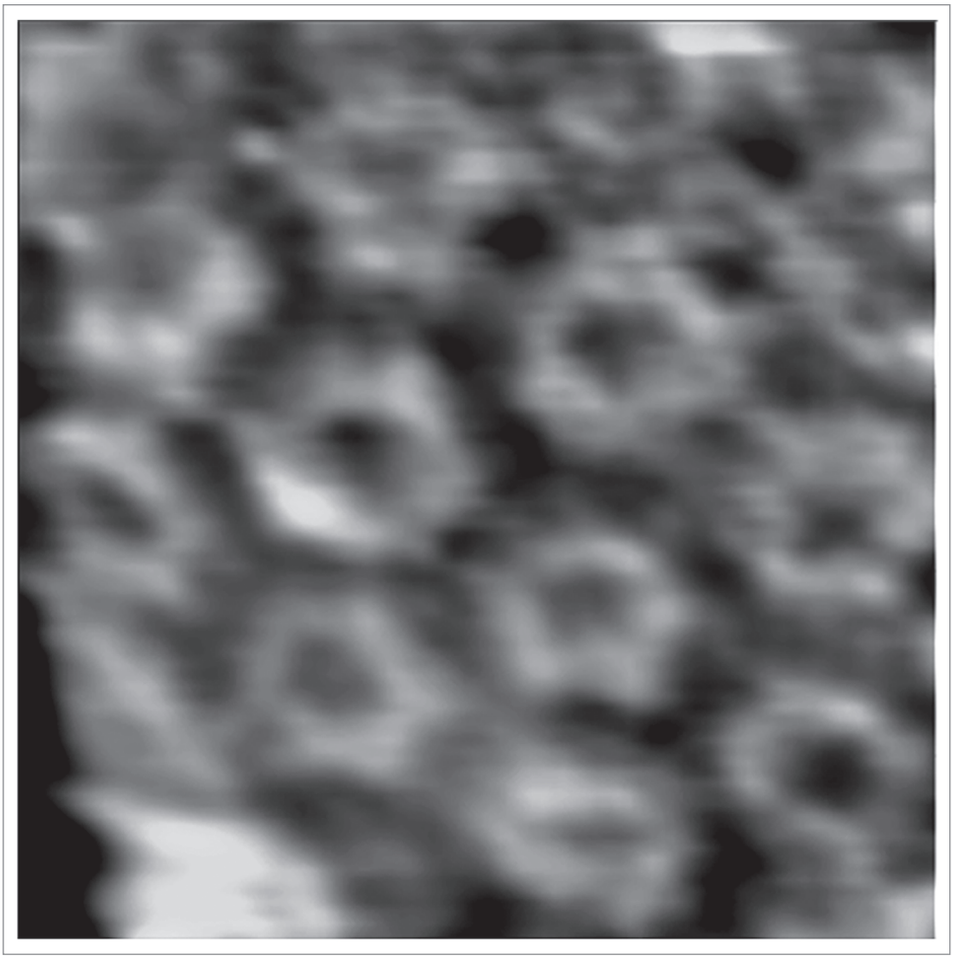

Figure 4. A high magnification AFM image of the head of a mutant T4 phage that fails to produce the hoc and soc proteins. The individual proteins that make up hexameric capsomeres are beginning to emerge. The depressions at the centers of the capsomeres that contain the binding sites for the surface proteins are clearly evident. The scan size is 50 nm x 50 nm and the height range is 100 nm.

but still comparable to the dimensions of intact capsids. The average heights of the objects were consistently about 8 nm with a standard deviation of 2.2 nm.

We believe the round objects seen in **Figure 5** to be empty phage capsids that have collapsed upon the substrate. They have not fractured as a result of osmotic shock, nor shattered upon drying, but spread like a deflated ball upon the substrate. The apparent perforations, or depressions are the centers of capsomeres, and indeed, the widths of these and their center to center distances of about 9 nm are consistent with those expected from the images of the icosahedral capsid and its distribution of capsomeres seen in **Figures 3a, b and 4**.

The round objects appear to be a disordered lattice of the doughnut shaped capsomeres of T4 that have spread like a thick fabric on the underlying mica. This observation is not without precedent. A similar icosahedrally derived fabric was seen in the AFM study of mimivirus[34] when its empty capsid collapsed. In that case the icosahedral arrangement of the capsomeres was relatively preserved; here the collapse appears to result in a cohesive but jumbled array of capsomeres that maintain their integrity in spite of the overall disorder. It may be noteworthy, that were the hoc and soc proteins still attached to the collapsed capsids, the observed depressions would not be visible to the AFM tip, as they are invisible on native capsids. Thus it appears that those proteins have detached from the collapsed and disordered heads.

Capsid dissolution into host cell membranes. **Figure 6a and b** contain remnants of cells that have been decimated by phage infection and lysis. Such images are somewhat perplexing as they include two structural formations. Around the periphery of the cell remnants are many phage attached to the cell surface through their tails and seen in profile. These, for the most part, have contracted tail sheaths and collapsed heads indicating that injection of DNA was triggered. On the planar surfaces of the cells, however, is a different scene. Here, as seen in **Figure 6**, we observe clusters of cusp shaped depressions of exactly the size of phage heads. In many cases, a tail assembly can be seen attached or associated with the edge of a cusp and lying parallel with the cell surface. The depressions present a variety of depths and detailed features. The most reasonable explanation is that the cusp shaped structures are empty phage heads that have collapsed and remain in direct contact with cell surfaces.

Phage DNA. We were able to promote emission of DNA from phage particles by osmotic shock while the virus was suspended in media, and in situ on the AFM substrate. We observed no virus with contracted sheaths having DNA emerging from the ends of tail assemblies. In **Figure 7** are AFM images of T4 DNA from particles osmotically shocked in their media and subsequently spread and dried on AFM substrates. In some images the DNA, though dispersed, is clearly still associated with individual T4 particles. The appearance of the DNA exhibits features in AFM images that we have come to associate with DNA that has no protein bound to it. Indeed, it has been reported that T4 DNA in the capsids is not associated with protein, but is closely packed and fills the entire head.[9,17,35,36] The appearance of the DNA is quite different than that which escapes from some larger DNA viruses such as PBCV-1,[37] vaccinia[38] and mimivirus[39] in which cases the DNA is extensively associated with protein molecules.

We also examined AFM images of DNA that had been cast onto the substrate by phage bound to the AFM substrate and ruptured in situ by washing with distilled water. Examples are seen in **Figure 8**. In most of these images the DNA is in the initial stages of spreading from the central bolus of nucleic acid. The DNA, as seen in the images of **Figure 8** is not present as separated, individual strands of double helical DNA as was seen for the most part in **Figure 7**, nor are the heights above the substrate, indicative of diameter, consistent with duplex DNA. Instead, as is evident in **Figure 8c and d**, threads composed of multiple duplex strands twisted about one another in complex arrangements are seen.

Assembly errors: Multiple tail assemblies. In **Figure 9** are examples of a rather common occurrence, phage particles having two complete tail assemblies. We would judge dual tailed phage make up two to three percent of the total virus present. The two tails always subtend an angle close to 72°, suggesting that they arise from two adjacent pentamers on the icosahedral head.

Discussion

Comparison with earlier studies based on electron microscopy. Although this is not the first AFM investigation of T4,[40,41] this is the first detailed, high-resolution AFM imaging of bacteriophage T4 and its structural components. We have, in previous papers, presented AFM studies of a range of different viruses,[42] but none exhibiting the asymmetry and level of architectural sophistication associated with tailed bacteriophage. Comparison of phage images obtained under fully hydrated conditions with those in air-dried samples indicate that shrinkage of larger moieties, such as the phage heads and tail assemblies, was 25% to 30%. This overall shrinkage is likely due not only to the loss of solvent, but also to compression as a result of drying forces. DNA, when dried, consistently exhibited heights above background of 1.5 to 1.7 nm. Because the A form of DNA (the dehydrated conformation) has a diameter of 2.5 nm, this implies a compression of roughly 30% at the molecular level as well.

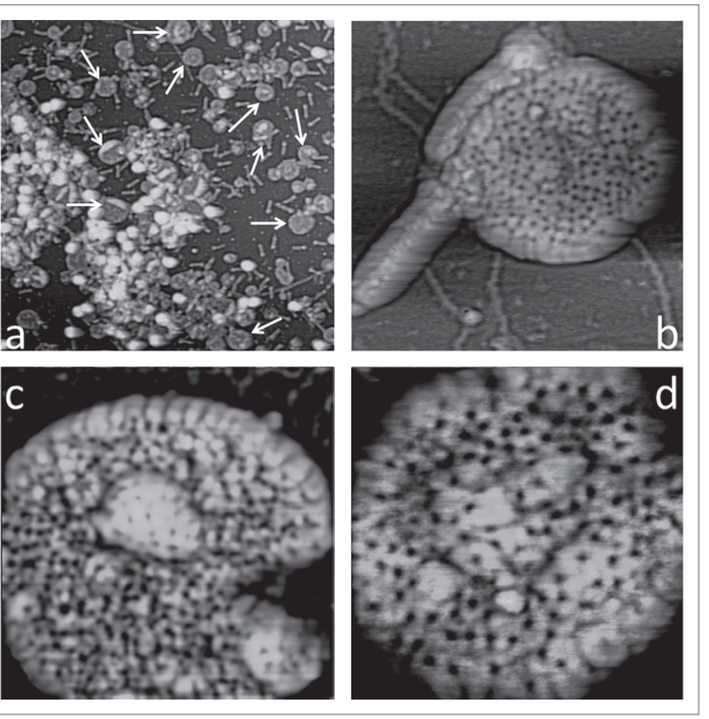

Figure 5. In (a) is a low magnification AFM image of the contents of a typical phage preparation that has undergone storage for about two years. It is characterized not only by intact phage and free tail assemblies, but also by disk shaped objects that appear to be permeated with holes or depressions of uniform size but in a disordered arrangement. The disks are frequently associated with a tail assembly as in (b). In (c and d) are high magnification AFM images of the disk shaped objects that we interpret as empty, collapsed phage capsids. The scan sizes and height ranges are (a) 3 μm x 3 μm, 150 nm, (b) 250 nm x 250 nm, 70 nm, (c) 250 nm x 250 nm, 30 nm and (d) 150 nm x 150 nm, 25 nm.

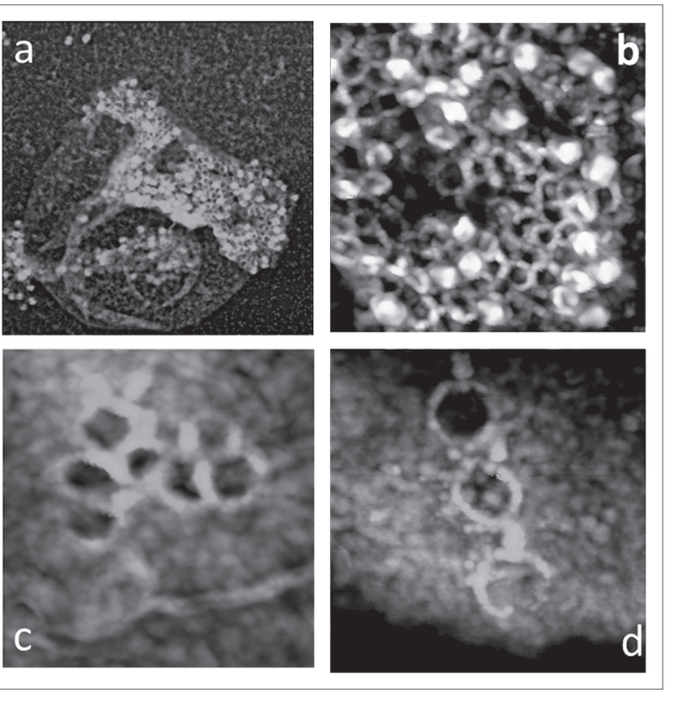

Figure 6. In (a) masses of phage particles are seen closely associated with a fragment of an *E. coli* cell. The particles are seen both in profile at the edges of the fragment and *en face* in the interior. In (b and c) are higher magnification images of the phage in direct contact with a cell surface, each particle appearing as a light rim (higher above the substrate) surrounding a dark (closer to the substrate) center. These are apparently phage heads that have collapsed into hemispheres, like deflated balls. Capsids are in direct contact with the membrane below. In (d) are three such particles on the surface of a cell membrane. That at top is the youngest to arrive and still exhibits the bottom of the "cup." That in the middle had arrived earlier and has seen its far side melt into the membrane or into the external media. The oldest arrival is at bottom and it has almost completely dissolved except for remnants of its rim. The scan areas and height ranges are respectively (a) 4 μm x 4 μm (b) 1 μm x 1 μm (c) 1 μm x 1 μm, 150 nm and (d) 500 nm x 500 nm, 100 nm.

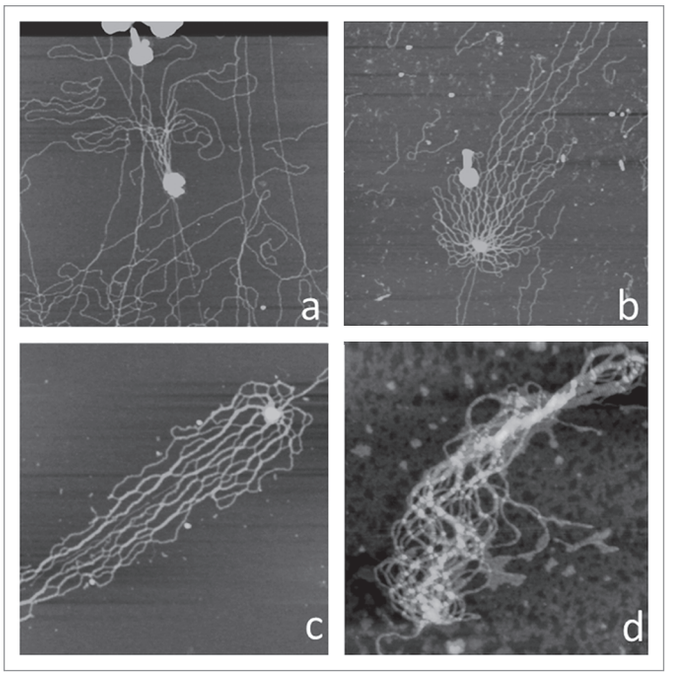

Figure 7. In (a) through (c) are phage heads ruptured by osmotic shock in solution (white objects because of their height far above the substrate) that have released their DNA and this has been spread across the AFM substrate. The flow direction is a consequence of washing the substrate with a directional stream of buffer. In (d) is a single bundle of phage DNA that constitutes the genome of a virus. In all of these images the DNA has had opportunity to unravel and spread, as the phage were disrupted in bulk solution and then applied to the AFM substrate. The scan sizes and height ranges are (a) 2 μm x 2 μm, 5 nm, (b) 2 μm x 2 μm, 5 nm, (c) 1 μm x 1 μm, 6 nm and (d) 1 μm x 1 μm, 10 nm.

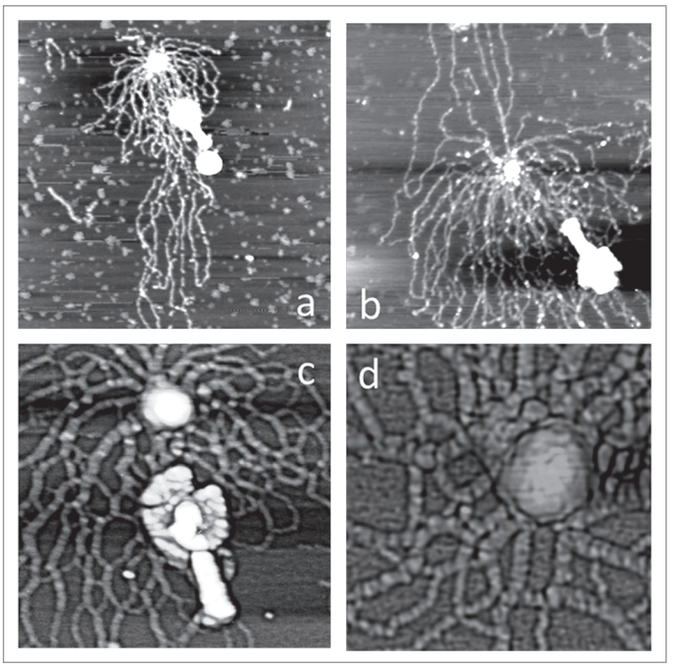

Figure 8. When phage particles were fixed to a mica substrate coated with poly-l-lysine and then exposed to distilled water, osmotic shock causes them to burst and release their bolus of condensed DNA immediately adjacent to the broken head. The DNA then begins to spread rather slowly over the substrate. In (a) through (c) the burst phage heads, bolus of DNA, and the spreading of the peripheral DNA is evident. In (d) is a higher magnification image of the DNA immediately adjacent to a newly released bolus of nucleic acid. The scan sizes and height ranges are (a) 1.5 μm x 1.5 μm, 5 nm, (b) 1 μm x 1 μm, 8 nm, (c) 500 nm x 500 nm, 30 nm and (d) 250 nm x 250 nm, 45 nm.

One of our objectives in examining a bacteriophage by AFM whose detailed structure has been well established by other techniques was to compare the qualitative and quantitative information that could be obtained by a relatively rapid AFM analysis with that yielded by electron microscopy. The results presented here suggest that the two methods are at least comparable, and in some regards the AFM results provide information immediately, such as the chirality of helixes, that is accessible to other methods only with a significantly greater investment of effort and resources. In particular, as increasingly larger viruses come under investigation, such as mimivirus,[39] the physical thickness of the virions becomes an obstacle to effective electron microscopy. Thickness, however, has no influence on AFM. Obviously AFM cannot reveal internal structure directly as can electron microscopy, but in terms of surface features and internal entities exposed as a consequence of specimen disruption, AFM provides images containing both unique and complementary information.

Additional observations from AFM. *Phage DNA.* T4 phage DNA, as illustrated by **Figures 7 and 8** is remarkably fluid with little perceptible segmental rigidity. The strands are often packed tightly against one another, suggesting that electrostatic repulsion is not severe. Evidence exists that when T4 infects an *E. coli*, the DNA may not spontaneously escape through the tail assembly due to internal pressure alone, but may be drawn into the host by activities internal to the cell.[23] AFM images also show that the DNA commonly exhibits acute turns and bends, occasionally forming almost hairpin structures. The contortions in the DNA backbone suggest that the flexibility and local variation in helix structure may be substantial. There have been earlier proposals based on solution X-ray diffraction, as well as electron microscopy, that DNA may be spooled within heads to form concentric shells.[43] In the AFM images of **Figures 7 and 8**, there is no order or regularity in the patterns of spilled DNA that lends support to that idea.

AFM images of DNA released from phage heads ruptured osmotically in situ are especially intriguing, as they show DNA as it is emerging from a packed form and beginning to spread. As seen in **Figure 8**, initially there is a roughly spherical bolus of highly condensed DNA that is expelled as a unit from the broken protein shell. Near the bolus, as DNA unravels and spreads, individual DNA strands are not seen, but thick, twisted cables of multistranded nucleic acid. This is evidenced by the measured thicknesses of the threads, as well as by the presence of numerous branch points, forks, and other instances where the threads break down into thinner strands.

The DNA exhibits a pronounced tendency to aggregate, and overall it has the appearance of a complex network of closely associated, possibly super coiled, multiple DNA strands. If the DNA

in T4 heads is indeed twisted about itself, or super coiled, then that conformation of the polymer represents stored energy generated by the expenditure of ATP upon DNA packaging. This energy, released upon unwinding and relaxation, might then be available to promote emission of DNA through the tail assembly at the time of infection.

Phage head dissolution. **Figure 6** contains AFM images of lysed *E. coli* cells exhibiting cusp shaped structures with distinctive depressions at their centers. The cusps consistently have exactly the diameters of T4 phage heads. Our interpretation of these images is that the cusp shaped features are phage particles that have lost their DNA and collapsed on the cell surface as a cup shaped shell. The collapsed phage heads subsequently dissolve from the bottoms of the cups. This explains the contrasting appearance of phage seen at the periphery compared with the interior phage heads in direct contact with a cell surface, the association of tails with the cusps, and the variation in the internal appearance of the cusps. In particular, **Figure 5d** shows three of these cusp structures closely positioned on a lysed cell surface. They represent three stages in the dissolution of capsid shells. The cusp at top is the newest collapsed phage particle to arrive, that in the middle an older associate, and the one at the bottom a particle that has nearly dissolved and exhibits only a gradually disappearing rim.

The explanation that we advance here implies that the major capsid proteins, and presumably the hoc and soc proteins, as well as other head associated proteins, either dissolve into the cell membrane remnants or, alternatively, are induced by contact with the cell membrane to dissolve into the surrounding media. The former possibility is most interesting. It is known that phage assembly occurs in association with the inside of the cell plasma membrane, and indeed, the capsid proteins may even emerge during assembly from a membrane environment. Thus dissolution into a membrane would not be unexpected.

Assembly anomalies. Smith and Trousdale first reported multi-tailed T4 phage particles in 1965 from electron micrographs.[44] Their work indicated that the multi-tailed phages could not be isolated as a pure strain and concluded, as do we, that they represent assembly errors and not genetic mutation. They further observed triple tailed T4 in much lower amounts, and even one particle that exhibited four tails.

While assembly errors of many sorts are probably not uncommon, this one is curious. Initiation of the assembly of a phage head is known to occur at a duodecameric ring of gp 20 proteins, the portal complex, that is anchored to the inside of the interior plasma membrane. Furthermore, the DNA must be ejected through the phage tail. This raises the questions of how there can be multiple nucleation points for head assembly, and how is it determined which tail assembly, if either, will be used for DNA emission.

The hoc and soc proteins. As shown by visualization of the hoc and soc minus mutant phage, the hoc and soc proteins are indeed flexible and do obscure the underlying capsomeres from the AFM tip. When they are absent, hexameric capsomeres consistent with previous observations and models appear. Whether the flexibility has functional significance, we cannot say. It does seem apparent, however, that due to their conformational instability, native phage particles constantly present different surface structures to their environment.

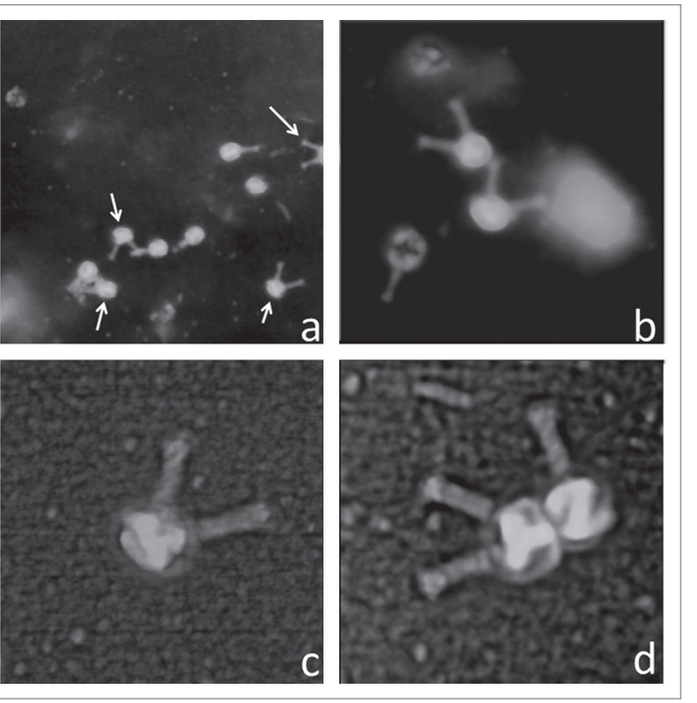

Figure 9. A common observation in our T4 preparations were phage particles having two tail assemblies oriented at the pentagonal angle of 72° to one another. In (a) are several examples of the multi tailed phage, indicated by arrows, seen in one 500 nm x 500 nm AFM image. They accounted for about 2% to 3% of the phage particles in some preparations. In (c) through (d) are multi tailed phage seen at higher magnification. The scan areas are (a) 2 μm x 2 μm, (b) 1 μm x 1 μm, (c) 500 nm x 500 nm and (d) 500 nm x 500 nm.

It should be noted that there may be a second explanation, or contributing factor to the features introduced by the two surface proteins. The proteins themselves are, of course, asymmetric, but they bind at a symmetry point at the centers of capsomeres. Hence the proteins can bind with any one of six different orientations at their binding sites. This means that there is 6-fold variability in the appearance of every capsomere with a hoc or soc protein bound. Presumably the orientation is random for each capsomere, hence the surface of virtually no phage particle is likely to be exactly the same as any other.

The sombrero shaped objects that we interpret as collapsed capsids appear to lack the hoc and soc proteins as well, though they are otherwise native. This is evident from the depressions visible at the centers of capsomeres, the usual binding sites for the surface proteins. It seems likely that the structural distortions imposed by capsid collapse disrupt the binding sites at the centers of the capsomeres and affect their release.

Materials and Methods

Bacteriophage T4 was prepared from infected *E. coli* cells as described in reference 6 and 45. AFM analyses[13,46] were generally performed in air, though in some cases scanning was performed

under buffer. In the latter case the buffer was 0.02 M HEPES at pH 7.0. The substrate was freshly cleaved mica, mica treated with magnesium chloride, or mica coated with poly-l-lysine. Nucleic acids usually adhered to magnesium treated surfaces carrying positive charges, while virus particles and their protein components usually adhered firmly to mica coated with poly-l-lysine. Most details of the AFM methods have been presented in earlier papers.[14,16,47-50]

Samples of 1.5 μl to 5 μl composed of neutral buffer and containing virus and viral components were applied to the substrate and allowed to sediment for 15 min to 30 min. The sample, on the substrate, was then exposed to 5% glutaraldehyde in buffer for 2 min and excess glutaraldehyde solution shaken off. The substrate was then washed two times with distilled water and dried in a stream of dry nitrogen gas. Alternatively, the sample, after sedimentation, was simply allowed to dry in air onto the substrate after excess liquid was removed on filter paper, and then fixed with glutaraldehyde.

Glutaraldehyde was necessary in most cases to rigidify biological samples sufficiently that they permitted scanning at high magnification. This is true of cells, viruses and large macromolecular complexes. Glutaraldehyde reacts with free amino groups of lysine residues of proteins, amino termini of proteins, and the exocyclic amino groups of nucleic acid bases adenine, guanine and cytosine.

Poly-l-lysine has proven to be a reliable adhesive for virtually all of the biological samples that we have investigated particularly cells, viruses and protein assemblies. While nucleic acids also adhere well to substrates coated with poly-l-lysine, the polymer produces a background level that often obscures the true heights of DNA and RNA. These protrude above the substrate only from 0.3 to 2.0 nm. Because nucleic acids also adhere well to substrates (mica, glass, plastic) treated with magnesium salts, such as magnesium chloride or magnesium acetate that don't produce a high background, those were the prefered substrates for visualization of RNA and DNA.

AFM imaging was performed using a Nanoscope III AFM instrument (Veeco Instruments, Santa Barbara, CA). When scanned in liquids, virus and associated macromolecules were scanned at 26°C using oxide—sharpened silicon nitride tips in a 75 μl fluid cell containing buffer. For scanning in air, silicon tips were employed. The images were collected in tapping mode[51,52] with an oscillation frequency of 9.2 kHz in fluid and 300 kHz in air, with a scan frequency of 1 Hz. Vertical and lateral distances were calibrated using standards from Digital Instruments (Santa Barbara, CA) of 10 nm height steps of pitch 200 nm, and standards from MCNC Analytical Labs with step height 10 nm and pitch of 1 μm. The AFM instrument was calibrated to small lateral distances by imaging the 111 face of a thaumatin protein crystal and using the known lattice spacings[53,54] as standard. Cantilevers for scanning in air were from Veeco (Santa Barbara, CA) and were TAP150 with lengths of 115–135 μm and spring constants of 5 Nn. For solution scanning, they were 0TR4 with lengths of 100 μm and spring constants of 0.08 Nn.

In the AFM images presented here, height above substrate is indicated by increasingly lighter color. Thus points very close to the substrate are dark and those well above the substrate white. Because lateral distances are distorted due to an AFM image being the convolution of the cantilever tip shape with the surface features scanned, quantitative measures of size were based either on heights above the substrate, or on center to center distances on particle surfaces.

Disclosure of Potential Conflicts of Interest

No potential conflicts of interest were disclosed.

Acknowledgements

We are grateful to Anastasia Aksyuk in Michael Rossmann's laboratory at Purdue University who provided us with native T4 phage samples and helpful instructions on how to propagate them, and to Professor Lindsay Black of the University of Maryland who graciously provided us with the hoc$^-$ and soc$^-$ T4 mutant phage as well as with a suppressor stain of *E. coli* on which to grow it. This research was supported in part by a grant to A.M. from the NIH, GM080412.

References

1. Ruska H. Die Sichbarmachtung der Bacteriophagen lyse im Ubermikroskop. Naturwissenschaften 1940; 28:45-52; http://dx.doi.org/10.1007/BF01486931.
2. Luria SE, Anderson TF. Identification and characterization of bacteriophages with the electron microscope. Proc Natl Acad Sci USA 1942; 28:127-30; PMID:16588529; http://dx.doi.org/10.1073/pnas.28.4.127.
3. Karam JD. Molecular Biology of Bacteriophage T4. American Assoc Microbiol Press. Washington DC 1994.
4. Matthews CK, Kutter EM, Mosig G, Berget PB. Bacteriophage T4. American Assoc. Washington DC: Microbiol Press 1983.
5. Mosig G, Eiserling F, Eds. T4 and related phages: structure and development. Oxford: Oxford Univ. Press, 2006.
6. Fokine A, Chipman PR, Leiman PG, Mesyanzhinov VV, Rao VB. Molecular architecture of the prolate head of bacteriophage T4. Proc Natl Acad Sci USA 2004; 101:6003-8; PMID:15071181; http://dx.doi.org/10.1073/pnas.0400444101.
7. Moore SD, Privelige PE. DNA packaging: a new class of molecular motors. Curr Biol 2002; 12:96; PMID:11839289; http://dx.doi.org/10.1016/S0960-9822(02)00670-X.
8. Sun S, Kondabagli K, Gentz PM, Rossmann MG, Rao VB. The structure of the ATPase that powers DNA packaging into bacteriophage T4 procapsids. Mol Cell 2007; 25:943-9; PMID:17386269; http://dx.doi.org/10.1016/j.molcel.2007.02.013.
9. Kindt J, Tzilil S, Ben-Shaul A, Gelbart WM. DNA packaging and ejection forces in bacteriophage. Proc Natl Acad Sci USA 2001; 98:13671-4; PMID:11707588; http://dx.doi.org/10.1073/pnas.241486298.
10. Wood WB, Crowther RA. Long Tail Fibers: Genes, Proteins, Assembly and Structure. In: Mathews CK, Kutter EM, Mosig G, Berget PB, Eds. Bacteriophage T4. Washington DC: Amer Soc Microbiology 1983; 259-69.
11. Black L, Showe MK. Morphogenesis of the T4 Head. In: Mathews CK, Kutter EM, Mosig G, Berget PB, Eds. Bacteriophage T4. Washington DC: Amer Soc Microbiology 1983; 219-45.
12. Ishii T, Yanagida M. The two dispensable structural proteins (soc and hoc) of the T4 phage capsid; their purification and properties, isolation and characterization of the defective mutants, and their binding with the defective heads in vitro. J Mol Biol 1977; 109:487-514; PMID:15127; http://dx.doi.org/10.1016/S0022-2836(77)80088-0.
13. Bustamante C, Keller D. Scanning force microscopy in biology. Phys Today 1995; 48:32-8; http://dx.doi.org/10.1063/1.881478.
14. Kuznetsov YG, Malkin AJ, Lucas RW, Plomp M, McPherson A. Imaging of viruses by atomic force microscopy. J Gen Virol 2001; 82:2025-34; PMID:11514711.
15. Kuznetsov YG, McPherson A. Atomic force microscopy in imaging of viruses and virus-infected cells. Microbiol Mol Biol Rev 2011; 75:268-85; PMID:21646429; http://dx.doi.org/10.1128/MMBR.00041-10.
16. Malkin AJ, Plomp M, McPherson A. Unraveling the Architecture of Viruses by High-Resolution Atomic Force Microscopy In: Lieberman PM, Ed. Virus Structure and Imaging, DNA Viruses, Methods and Protocols. Totowa, New Jersey: Humana Press 2004; 85-108.

17. Calalano E. Viral Genome Packaging Machines: Genetics, Structure and Mechanism. New York, NY: Kluwer Academic/Plenum Publishers 2005.
18. Eiserling FA. Structure of the T4 Virion. In: Matthews CK, Mosig G, Berget PB, Ed. Bacteriophage T4. Washington DC: Amer Soc Microbiol 1983; 11-24.
19. Parker SD, Wall JS, Hunter E. Analysis of mason-pfizer monkey virus Gag particles by scanning transmission electron microscopy. J Virol 2001; 75:9543-8; PMID:11533218; http://dx.doi.org/10.1128/JVI.75.19.9543-8.2001.
20. Earnshaw WC, King J, Eiserling FA. The size of the bacteriophage T4 head in solution with comments about the dimension of virus particles as visualized by electron microscopy. J Mol Biol 1978; 122:247-53; PMID:682194; http://dx.doi.org/10.1016/0022-2836(78)90040-2.
21. Eiserling FA, Black LW. Molecular Biology of Bacteriophage T4.s. In: Karam JD, Ed. Washington DC: American Soc Microbiol 1994.
22. Berget PB, King J. T4 Tail Morphogenesis. In: Mathews CK, Kutter EM, Mosig G, Berget PB, Eds. Bacteriophage T4 Washington DC: Amer Soc Microbiology 1983; 246-58.
23. Goldberg E. Recognition, Attachment and Injection. In: Mathews CK, Kutter EM, Mosig G, Berget PB, Eds. Bacteriophage T4 Washington DC: Amer Soc Microbiology 1983; 32-9.
24. Kuznetsov YG, Martiny JB, McPherson A. Structural analysis of a Synechococcus myovirus S-CAM4 and infected cells by atomic force microscopy. J Gen Virol 2010; 91:3095-104; PMID:20739271; http://dx.doi.org/10.1099/vir.0.025254-0.
25. Amos LA, Klug A. Three dimensional image reconstruction of the contractile tail of the T4 bacteriophage. J Mol Biol 1975; 99:51-64; PMID:1206701; http://dx.doi.org/10.1016/S0022-2836(75)80158-6.
26. Caspar DL. Movement and self-control in protein assemblies. Quasi-equivalence revisited. Biophys J 1980; 32:103-38; PMID:6894706; http://dx.doi.org/10.1016/S0006-3495(80)84929-0.
27. Coombs DH, Eiserling FA. Studies on the structure, protein composition and aseembly of the neck of bacteriophage T4. J Mol Biol 1977; 116:375-405; PMID:592389; http://dx.doi.org/10.1016/0022-2836(77)90076-6.
28. Kellenberger E, Arber W. Die Structure des Schwanges der Phagen T2 and T4 und der Mechanismes der irreversiblen Absorbtion. Z Naturforsch Teil 1955; 10:698-704.
29. Aebi U, van Driel R, Bijlenga RK, ten Heggeler B, van den Brock R, Steven AC, et al. Capsid fine structure of T-even bacteriophages. Binding and localization of two dispensable capsid proteins into the P23* surface lattice. J Mol Biol 1977; 110:687-98; PMID:859178; http://dx.doi.org/10.1016/S0022-2836(77)80084-3.
30. Moody MF. The shape of the T-even bacteriophage head. Virology 1965; 26:567-76; PMID:5833315; http://dx.doi.org/10.1016/0042-6822(65)90319-3.
31. Moody MF, Makowski L. X-ray diffraction study of tail-tubes from bacteriophage T2L. J Mol Biol 1981; 150:217-44; PMID:7321045; http://dx.doi.org/10.1016/0022-2836(81)90450-2.
32. Baschong W, Aebi U, Baschong-Prechianotto C, Dubochet J, Landmann L, Kellenberger E, et al. Head structure of bacteriophages T2 and T4. J Ultrastruct Mol Struct Res 1988; 99:189-202; PMID:3198952; http://dx.doi.org/10.1016/0889-1605(88)90063-8.
33. Yanagida M. Molecular organization of the shell of T-even bacteriophage head. II. Arrangement of subunits in the head shell of giant phages. J Mol Biol 1977; 109:515-37; PMID:845938; http://dx.doi.org/10.1016/S0022-2836(77)80089-2.
34. Kuznetsov YG, Xiao C, Sun S, Raoult D, Rossmann M, McPherson A. Atomic force microscopy investigation of the giant mimivirus. Virology 2010; 404:127-37; PMID:20552732; http://dx.doi.org/10.1016/j.virol.2010.05.007.
35. Casjens S. Principles of Virion Structure, Function and Assembly. In: Chu W, Burnett RM, Garcea R, Eds. Structural Biology of Viruses. Oxford, UK: Oxford Univ Press 1997.
36. Rao VB, Black LW, Eds. DNA packaging in bacteriophage T4. New York NY: Kluwer Academic Plenum 2005.
37. Kuznetsov YG, Gurnon JR, Van Etten JL, McPherson A. Atomic force microscopy investigation of a chlorella virus, PBCV-1. J Struct Biol 2005; 149:256-63; PMID:15721579; http://dx.doi.org/10.1016/j.jsb.2004.10.007.
38. Kuznetsov Y, Gershon PD, McPherson A. Atomic force microscopy investigation of vaccinia virus structure. J Virol 2008; 82:7551-66; PMID:18508898; http://dx.doi.org/10.1128/JVI.00016-08.
39. Xiao C, Kuznetsov YG, Sun S, Hafenstein SL, Kostyuchenko VA, Chipman PR, et al. Structural studies of the giant mimivirus. PLoS Biol 2009; 7:92; PMID:19402750; http://dx.doi.org/10.1371/journal.pbio.1000092.
40. Matsko N, Klinov D, Manykin A, Demin V, Klimenko S. Atomic force microscopy analysis of bacteriophage phiKZ and T4. Jap Soc Elec Micros 2001; 50:417-22; http://dx.doi.org/10.1093/jmicro/50.5.417.
41. Ikai A, Yoshimura K, Arisaka F, Ritani A. Atomic force microscopy of bacteriophage T4 and its tube-baseplate complex. FEBS Lett 1993; 326:39-41; PMID:8325385; http://dx.doi.org/10.1016/0014-5793(93)81756-P.
42. Stepanenko OV, Fonin AV, Morozova KS, Verkhusha VV, Kuznetsova IM, Turoverov KK, et al. New Insight in Protein-Ligand Interactions. 2. Stability and Properties of Two Mutant Forms of the d-Galactose/d-Glucose-Binding Protein from *E. coli*. J Phys Chem B 2011; 115:9022-32; PMID:21671572; http://dx.doi.org/10.1021/jp204555h.
43. Earnshaw WC, King J, Harrison SC, Eiserling FA. The structural organization of DNA packaged within the heads of T4 wild-type, isometric and giant bacteriophages. Cell 1978; 14:559-68; PMID:688382; http://dx.doi.org/10.1016/0092-8674(78)90242-8.
44. Smith KO, Trousdale M. Multiple-Tailed T4 Bacteriophage. J Bacteriol 1965; 90:796-802; PMID:16562083.
45. Kellenberger E. Studies on the morphopoiesis of the head of phage T-even. V. The components of the T4 capsid and of other, capsid-related structures. Virology 1968; 34:549-61; PMID:4870477; http://dx.doi.org/10.1016/0042-6822(68)90074-3.
46. Binnig G, Quate CF. Atomic force microscope. Phys Rev Lett 1986; 56:930-3; PMID:10033323; http://dx.doi.org/10.1103/PhysRevLett.56.930.
47. Kuznetsov YG, Daijogo S, Zhou J, Semler BL, McPherson A. Atomic force microscopy analysis of icosahedral virus RNA. J Mol Biol 2005; 347:41-52; PMID:15733916; http://dx.doi.org/10.1016/j.jmb.2005.01.006.
48. Kuznetsov YG, Datta S, Kothari NH, Greenwood A, Fan H, McPherson A. Atomic force microscopy investigation of fibroblasts infected with wild-type and mutant murine leukemia virus (MuLV). Biophys J 2002; 83:3665-74; PMID:12496133; http://dx.doi.org/10.1016/S0006-3495(02)75366-6.
49. Kuznetsov YG, Victoria JG, Low A, Robinson WE Jr, Fan H, McPherson A. Atomic force microscopy imaging of retroviruses: human immunodeficiency virus and murine leukemia virus. Scanning 2004; 26:209-16; PMID:15536976; http://dx.doi.org/10.1002/sca.4950260409.
50. Kuznetsov YG, McPherson A. Identification of DNA and RNA from retroviruses using ribonuclease A. Scanning 2006; 28:278-81; PMID:17063767; http://dx.doi.org/10.1002/sca.4950280506.
51. Hansma HG, Hoh JH. Biomolecular imaging with the atomic force microscope. Annu Rev Biophys Biomol Struct 1994; 23:115-39; PMID:7919779; http://dx.doi.org/10.1146/annurev.bb.23.060194.000555.
52. Hansma HG, Pietrasanta L. Atomic force microscopy and other scanning probe microscopies. Curr Opin Chem Biol 1998; 2:579-84; PMID:9818182; http://dx.doi.org/10.1016/S1367-5931(98)80086-0.
53. Ko TP, Day J, Greenwood A, McPherson A. Structures of three crystal forms of the sweet protein thaumatin. Acta Crystallogr D Biol Crystallogr 1994; 50:813-25; PMID:15299348; http://dx.doi.org/10.1107/S0907444994005512.
54. Kuznetsov Yu G, Malkin AJ, McPherson A. AFM studies on the mechanisms of nucleation and growth of macromolecular crystals. J Cryst Growth 1999; 196:489-502; http://dx.doi.org/10.1016/S0022-0248(98)00856-2.